Endothelial cell protein C receptor cellular localization and trafficking: potential functional implications

Ramesh C. Nayak,[1] Prosenjit Sen,[1] Samit Ghosh,[1] Ramakrishnan Gopalakrishnan,[1] Charles T. Esmon,[2] Usha R. Pendurthi,[1] and L. Vijaya Mohan Rao[1]

[1]Center for Biomedical Research, University of Texas Health Science Center at Tyler; and [2]Cardiovascular Biology Research Program, Oklahoma Medical Research Foundation, and Howard Hughes Medical Institute, Oklahoma City

Although the binding of endothelial cell protein C receptor (EPCR) to its ligands is well characterized at the biochemical level, it remains unclear how EPCR interaction with its ligands at the cell surface impacts its cellular trafficking. We characterized the cellular localization and trafficking of EPCR in endothelial cells and a heterologous expression system. Immunofluorescence confocal microscopy studies revealed that a majority of EPCR is localized on the cell surface in membrane microdomains that are positive for caveolin-1. A small fraction of EPCR is also localized intracellularly in the recycling compartment. Factor VIIa (FVIIa) or activated protein C binding to EPCR promoted the internalization of EPCR. EPCR and EPCR-bound ligands were endocytosed rapidly via a dynamin- and caveolar-dependent pathway. The endocytosed receptor-ligand complexes were accumulated in a recycling compartment before being targeted back to the cell surface. EPCR-mediated FVIIa endocytosis/recycling also resulted in transport of FVIIa from the apical to the basal side. In vivo studies in mice showed that blockade of EPCR with EPCR-blocking antibodies impaired the early phase of FVIIa clearance. Overall, our results show that FVIIa or activated protein C binding to EPCR promotes EPCR endocytosis, and EPCR-mediated endocytosis may facilitate the transcytosis of FVIIa and its clearance from the circulation. (Blood. 2009; 114:1974-1986)

Introduction

Endothelial cell protein C receptor (EPCR) is a cellular receptor for protein C and activated protein C (APC).[1] It is primarily localized on the endothelial cells of large blood vessels and is very low or absent from the microvascular endothelium of most tissues.[2] Protein C binding to EPCR increases the rate of protein C activation by thrombin-thrombomodulin complexes.[3] EPCR, in addition to controlling the coagulation by modulating protein C-mediated anticoagulant pathway, has been shown to play an important role in many pathophysiologic processes, such as inflammation responses to infection and trauma, hematopoiesis, and autoimmunity.[4] Recent studies suggest that APC bound to EPCR activates protease-activated receptor-mediated cell signaling, and this may be responsible for some of the nonhemostatic functions of EPCR.[5-8]

Our recent studies of factor VIIa (FVIIa) binding to endothelial cells revealed that EPCR also serves as a receptor for FVII and FVIIa on the endothelium.[9] In parallel studies, Preston et al[10] also found that FVIIa bound to soluble EPCR with a comparable affinity as of protein C. FVIIa binding to EPCR appeared to have no measurable consequences on FVIIa coagulant or cell signaling activities.[9] However, therapeutic concentrations of FVIIa, by competing with protein C and APC binding to EPCR, impaired EPCR-dependent protein C activation and APC-mediated cell signaling, respectively. More importantly, EPCR mediated the internalization of FVIIa bound to it on cell surfaces, indicating that EPCR may play a role in FVIIa clearance.[9]

Although much is known about the biochemistry of EPCR and its interaction with protein C/APC, there is little information on how EPCR expression is regulated at the cell surface. It had been suggested that EPCR is homologous and probably identical to intracellular murine protein, CCD41, a centrosomal protein.[11] Posttranslational modification of EPCR/CCD41 gene product was shown to be responsible whether the protein is directed to the cell surface or the centrosome.[11] However, there were no other reports in the literature confirming this finding. At present, there is no information on intracellular distribution of human EPCR. Further, it is unclear how FVIIa or APC binding to EPCR modulates its cellular expression and the pathways by which EPCR mediates the internalization of FVIIa or APC.

In the present study, we characterized the cellular localization of EPCR in endothelial cells and CHO cells stably transfected with EPCR, mode of EPCR-mediated endocytosis, and intracellular trafficking of the internalized ligands and the receptor.

Methods

Reagents

Mouse monoclonal antibodies (mAbs) against human EPCR (JRK-1494/blocking mAb and JRK-1500/nonblocking mAb) were prepared as described earlier.[3] mAbs against mouse EPCR (mAb 1560/blocking mAb and mAb 1567/nonblocking mAb) were prepared by immunizing rats with recombinant mouse soluble EPCR.[12] Antibodies against early endosomal marker rab5 and EEA1 were obtained from Santa Cruz Biotechnology. Anti-LAMP1 and anti-Giantin antibodies were purchased from Abcam, and anti-rab11 was from Zymed Laboratory. Secondary antibodies conjugated

Submitted March 4, 2009; accepted June 22, 2009. Prepublished online as *Blood* First Edition paper, July 8, 2009; DOI 10.1182/blood-2009-03-208900.

The online version of this article contains a data supplement.

The publication costs of this article were defrayed in part by page charge payment. Therefore, and solely to indicate this fact, this article is hereby marked "advertisement" in accordance with 18 USC section 1734.

with Oregon Green or Rhodamine Red and AlexaFluor 488 (AF488) labeling kit and anti-AF488 antibodies were obtained from Invitrogen. FVII was purified from plasma as described earlier,[13] and protein C was obtained from Enzyme Research Laboratories. Recombinant human FVIIa was from Novo Nordisk A/S, and recombinant activated protein C (Xigris) was from Eli Lilly.

Cell culture

Primary human umbilical vein endothelial cells (HUVECs) and EBM-2 basal medium and growth supplements were purchased from Lonza. Endothelial cells were cultured in EBM-2 basal medium supplemented with growth supplements, 1% penicillin/streptomycin and 5% fetal bovine serum. Generation of CHO cells stably expressing EPCR (CHO-EPCR) was described previously.[9] Both wild-type and CHO-EPCR cells were cultured in Ham's F12 medium containing 1% penicillin/streptomycin and supplemented with 10% fetal bovine serum.

Plasmid constructs

Wild-type rab11, and its constitutive active (rab11 Q70L) and dominant negative form (rab11 S25N), cloned in pCDNA3.1 mammalian expression vector was kindly provided by David Sabatini (New York University School of Medicine). Human EPCR cDNA cloned in pZeoSV (pZeoSC-EPCR219)[14] was used as template to generate full-length EPCR cDNA and EPCR cDNA lacking 45 bp (signal peptide sequence) at its N-terminus by polymerase chain reaction amplification (for more information on plasmid constructs and other methods, see supplemental data, available on the *Blood* website; see the Supplemental Materials link at the top of the online article).

Radiolabeling

FVIIa and APC were labeled with ^{125}I using Iodogen (Pierce Chemical)-coated polypropylene tubes and Na^{125}I (PerkinElmer Life and Analytical Sciences) according to the manufacturer's technical bulletin and as described previously.[15,16]

Fluorescent probe labeling

FVIIa and other EPCR ligands were labeled with AF488 using the AF488 labeling kit and following the instructions provided in the manufacturer's technical bulletin (Invitrogen). Approximately 100 μg of protein was used for each labeling. The degree of labeling (moles dye/mole protein) was very similar (3.7-4.0) among the labeled proteins.

Cell surface biotinylation and EPCR endocytosis

Biotinylation of cell surface proteins with NHS-S-S-biotin was performed as described earlier.[17] The biotin-labeled cells were exposed to control vehicle, FVIIa, or APC in buffer B (10 mM N-2-hydroxyethylpiperazine-N′-2-ethanesulfonic acid, 0.15 M NaCl, 4 mM KCl, 11 mM glucose, pH 7.4 [buffer A] containing 1 mg/mL bovine serum albumin [BSA] and 5 mM $CaCl_2$) for various times at 37°C. After the treatment, the cells were washed with phosphate-buffered saline (PBS), and the cell surface biotin was cleaved by incubating them with a cell-impermeable reducing buffer (50 mM glutathione, 1 mM $MgCl_2$, 1.0 mM ethylenediaminetetraacetic acid, 0.2% BSA, and 75 mM NaCl, pH 8.0) for 10 minutes at 37°C. The cells were then washed with PBS and lysed in 200 μL lysis buffer (20 mM Tris-HCl, pH 7.4, containing 1 mM ethylenediaminetetraacetic acid, 150 mM NaCl, 1% Triton X-100, and a cocktail of protease inhibitors), and the cell lysates were processed for EPCR immunoprecipitation.

Immunoprecipitation and Western blotting

Cell lysates were incubated overnight at 4°C with EPCR mAb (JRK1496, 10 μg), followed by protein A/G agarose beads (20 μL) for 4 hours. After the removal of the cell lysate by centrifugation, the beads were washed 3 times with 10 mM N-2-hydroxyethylpiperazine-N′-2-ethanesulfonic acid buffer to remove the unbound material, and the bound material was eluted with 50 μL sodium dodecyl sulfate-polyacrylamide gel electrophoresis (SDS-PAGE) sample buffer. Eluted samples (15 μL) were subjected to SDS-PAGE, followed by immunoblot analysis with streptavidin-horseradish peroxidase conjugate.

Disruption of caveolae- and coated-pit pathway-mediated internalization

For disruption of caveolae, the cells were treated with methyl-β-cyclodextrin (mβCD; 10 mM) for 30 minutes. To inhibit the clathrin-coated pit pathway of internalization, the cells were rinsed in K^+ free buffer (20 mM N-2-hydroxyethylpiperazine-N′-2-ethanesulfonic acid, 140 mM NaCl, 5 mM $CaCl_2$, 1 mM $MgCl_2$, and 1 mg/mL D-glucose) and then incubated for 5 minutes in hypotonic K^+ free buffer (K^+ free buffer diluted 1:1 with distilled water). The cells were again rinsed and incubated for 20 minutes in K^+ free buffer before adding ligands to the cells. For controls, cells were treated identically except that all buffer solutions contained 10 mM KCl.

Radioactivity-based internalization, degradation, and recycling assays

Internalization and degradation of ^{125}I-labeled FVIIa and other ligands were determined as described recently.[9] To determine recycling of the internalized ligands, ^{125}I-labeled ligands (10 nM) in buffer B were incubated with CHO-EPCR cells for 2 hours at 37°C to allow EPCR-mediated internalization. After 2 hours of incubation, the unbound ligand was removed, the cells were washed with buffer B, and the cell surface-associated ligand was eluted by treating the cells with 0.1 M glycine (pH 2.3) for 3 minutes. Thereafter, the cells were washed twice with buffer B and allowed to stand in buffer B at 37°C. At various time intervals, the overlying buffer was removed and counted for the radioactivity.

Immunofluorescence-based internalization and recycling assays

Cells cultured on glass coverslips were incubated with FVIIa or other EPCR ligands (50 nM) that were tagged with fluorescent dye AF488 on ice-bath for 1 hour to allow the binding of the ligand to EPCR with no or minimal internalization of the bound ligand. At the end of a 1-hour incubation, the unbound ligand was removed, and the cells were washed once with cold buffer B and then were warmed to 37°C to induce the internalization. At various time intervals, the cells were fixed, permeabilized, and processed for immunofluorescence confocal microscopy. For steady-state internalization studies, HUVECs or CHO-EPCR cells were incubated at 37°C for various time periods with AF488-FVIIa or other AF488-conjugated ligands (50 nM). To monitor the endocytic pathway of FVIIa or APC, CHO-EPCR cells grown on glass coverslips were exposed to both AF488-FVIIa (or AF488-APC; 50 nM) and AF555-transferrin (300 nM) simultaneously for 5, 15, and 30 minutes. At the end of each time point, the cells were washed with cold buffer B and processed for immunofluorescence confocal microscopy. To monitor the recycling of the internalized ligands, CHO-EPCR cells were first incubated with AF488-conjugated FVIIa or APC (50 nM) for 1 hour at 37°C; then the bound ligand was removed by washing the cells with buffer A containing 5 mM ethylenediaminetetraacetic acid, and the cells were washed with buffer B and allowed to stay in buffer B at 37°C. After various times at 37°C, the cells were fixed and processed for immunofluorescence confocal microscopy.

Immunofluorescence microscopy

The cells cultured on glass coverslips, control, or exposed to FVIIa or other ligands were washed first in buffer B and then fixed for 1 hour at 4°C in PBS containing 4% paraformaldehyde. The fixative was removed, and the extra formaldehyde was quenched with 0.05% glycine, pH 8.0, for 5 minutes. The fixed cells were either permeabilized with 0.1% Triton X-100 in PBS for 10 minutes or left nonpermeabilized and blocked with 3% goat serum in PBS for 1 hour at room temperature. Both nonpermeabilized and permeabilized cells were treated with EPCR monoclonal antibody (JRK-1500; 10 μg/mL) and/or rabbit polyclonal antibody for different organelle markers (2-5 μg/mL) overnight at 4°C. After removing the unbound primary antibodies and washing them twice with PBS, the cells were

incubated with Oregon Green-conjugated (excitation/emission wavelength 496/524 nm) or Rhodamine Red-conjugated (excitation/emission wavelength, 570/590 nm) anti–rabbit or anti–mouse IgG (4 μg/mL) for 60 minutes at room temperature. The cells were washed and the coverslips were mounted on a glass slide using aqueous gel mounting media (Biomedia) containing antifading agent.

Image acquisition, scoring, and colocalization

Most of the immunostained cells were viewed using a Nikon Eclipse TE2000-S inverted microscope using Plan Apo 60×/1.40 oil objective lens. The confocal images were acquired using Ultra*VIEW* LCI confocal system (PerkinElmer) as described recently.[17,18] Images were scanned using 488 nm excitation laser line for Oregon Green and AF488, and 543 nm excitation laser line for Rhodamine Red-X and AF555 dyes. A digital CCD camera (C4742-95-12ERG; HAMAMATSU Photonics), was used to capture the images. PerkinElmer ImagingSuite (Version 5.2) acquisition and processing software was used for the acquisition of images, determining colocalization, and quantifying the signal (counting pixel value). Some of the confocal images (Figure 1A, top 2 panels of Figure 1C, bottom panel of Figure 1G, Figure 2, and Figure 3A) were obtained using LSM 510 Meta confocal system (Carl Zeiss) equipped with an inverted microscope (Axio Observer Z1; Carl Zeiss). Immunostained cells were viewed using Plan-APOCHROMAT 63×/1.4 NA oil objective lens. Argon ion 488 nm laser line was used for the excitation of Oregon Green and AF488, and HeNe 543 nm laser line for the excitation of Rhodamine Red-X and AF555. Diode 405-30 laser line was used to scan images for DAPI. Zen 2007 software (Carl Zeiss) was used for the image acquisition. The scanned images were exported and processed using Adobe Photoshop Version 7.0 software (Adobe Systems).

Transcytosis of FVIIa

CHO, CHO-EPCR, or HUVECs were seeded onto gelatin-coated (0.1 mg/mL for 10 minutes) membrane of the upper chamber of transwells (25 000 cells, 10 000 cells in case of HUVECs)/12-mm-diameter dish, polycarbonate membrane, 3 μm pore size, Corning) and cultured for 5 days to form tight confluent monolayers. ^{125}I-FVIIa (10 nM) and BSA labeled with Evans Blue (0.67 mg/mL) were added to the upper chamber in 0.5 mL of medium. At various times, a small aliquot was removed from the lower chamber (contains 1.5 mL of medium) and counted for the radioactivity to quantify FVIIa levels or measured absorbance at 650 nm to measure BSA levels. To determine EPCR-specific transcytosis, CHO-EPCR cells were treated with control vehicle or EPCR blocking antibody (JRK 1494, 10 μg/mL) for 30 minutes before adding ^{125}I-FVIIa and Evans Blue-BSA to the upper chamber, and the difference in the radioactivity transported across CHO-EPCR cells treated with control vehicle or the blocking antibody was taken as EPCR-mediated specific transcytosis. No significant differences were noted in the transport of Evans Blue BSA in CHO-EPCR cells treated with control vehicle or EPCR blocking antibodies.

In vivo distribution of factor VII and protein C

All studies involving animals were conducted in accordance with the animal welfare guidelines set forth in the Guide for the Care and Use of Laboratory Animals and Department of Health and Human Services. All animal procedures were approved by the Institutional Animal Use and Care Committee of the University of Texas Health Science Center at Tyler. AF488-labeled human FVII or protein C was administered into anesthetized male C57BL/6 mice through tail vein (10 μg/mouse in 100 μL of saline). After one hour, the mice were killed by exsanguination. Various organs were collected and fixed in Excel fixative. After overnight fixation, the tissues were processed and stained with rabbit anti-AF488 antibodies and developed using 3-amino-9-ethylcarbazole substrate chromogen (Dako North America) and counterstained with hematoxylin. The stained tissue sections were viewed with an OLYMPUS BX41 upright microscope using U Plan FI 40×/0.75 objective lens and the images were captured with an OLYMPUS DP25 digital CCD camera using DP2-BSW software. The images were processed and arranged using Adobe Photoshop Version 7.0 software.

FVIIa clearance in mice

^{125}I-FVIIa (5 μg/kg body weight) was injected into C57/BL6 mice under anesthesia through tail vein (intravenously in 100 μL volume). Before injecting ^{125}I-FVIIa, mice were treated with control vehicle, EPCR nonblocking (mAb 1567), or EPCR blocking (mAb 1560) antibodies (the antibodies were administered intraperitoneally 30 minutes before the injection of ^{125}I-FVIIa and intravenously along ^{125}I-FVIIa, 50 μg antibody/mouse at each time). Immediately after the injection of ^{125}I-FVIIa and at a predefined interval, 50 μL of blood was collected from orbital sinus, and the amount of radioactivity in plasma was counted. The radioactivity counts present in the plasma obtained immediately after the injection was taken as 100%.

Results

Cellular distribution of EPCR

The surface and intracellular distribution of EPCR in endothelial cells and CHO cells stably transfected with EPCR was characterized by immunofluorescence confocal microscopy. As expected, EPCR mAbs brightly stained the cell surface of both nonpermeabilized and permeabilized endothelial cells (Figure 1A). EPCR was distributed at the cell surface in a patchy or punctuate manner (supplemental Figure 1). Analysis of Z-stack images showed that EPCR was distributed evenly on the entire cell surface with no evidence for preferential sorting to either apical or basolateral surfaces (data not shown). The status of cell confluence had no detectable effect on EPCR expression and localization (supplemental Figure 1). In permeabilized endothelial cells, EPCR staining was also observed intracellularly, mostly around perinuclear region and some in dispersed dots throughout the cytoplasm (Figure 1A). In CHO-EPCR cells, EPCR intracellular staining was noted predominantly in single discreet intense patch at the juxtanuclear region of the cell and few small, dispersed dot-like structures in the cytoplasm beneath the plasma membrane (Figure 1B). When EPCR mAb was replaced with nonimmune mouse IgG, no fluorescence signal was detected in either nonpermeabilized or permeabilized HUVECs or CHO-EPCR cells. Similarly, no fluorescence signal was detected if wild-type CHO cells were stained with EPCR mAb (data not shown).

To investigate whether the patchy or punctuate distribution of EPCR on the cell surface reflects EPCR localization in specialized membrane microdomains, such as caveolae, HUVECs and CHO-EPCR were stained with antibodies against EPCR and caveloin-1, the core protein of caveolae. Both EPCR and caveolin-1 were stained intensely at the cell surface of both the cell types and the overlap of EPCR, and caveolin-1 immunofluorescence showed a high degree of colocalization (correlation coefficient of 0.866 ± 0.015, $n = 10$ and 0.945 ± 0.009, $n = 10$ in CHO-EPCR cells and HUVECs, respectively). Removal of membrane cholesterol from the plasma membrane by mβCD treatment, which disrupts caveolae and lipid rafts, led to uniform and smooth distribution of EPCR on the cell surface and markedly reduced the colocalization of EPCR and caveolin-1 (Figure 1C).

Because EPCR was localized in a dense cytoplasmic globular spot at a perinuclear position, an expected site of the centrosome, we tested whether EPCR localization at this vicinity represents the posttranslational modified, signal peptide-deleted EPCR localization in the centrosome as reported earlier.[11] Wild-type CHO cells were transfected transiently with plasmid constructs expressing a full-length EPCR or EPCR lacking 15 amino acids at N-terminus (signal peptide; ΔspEPCR) tagged with GFP at the C-terminus. The GFP fusion product of

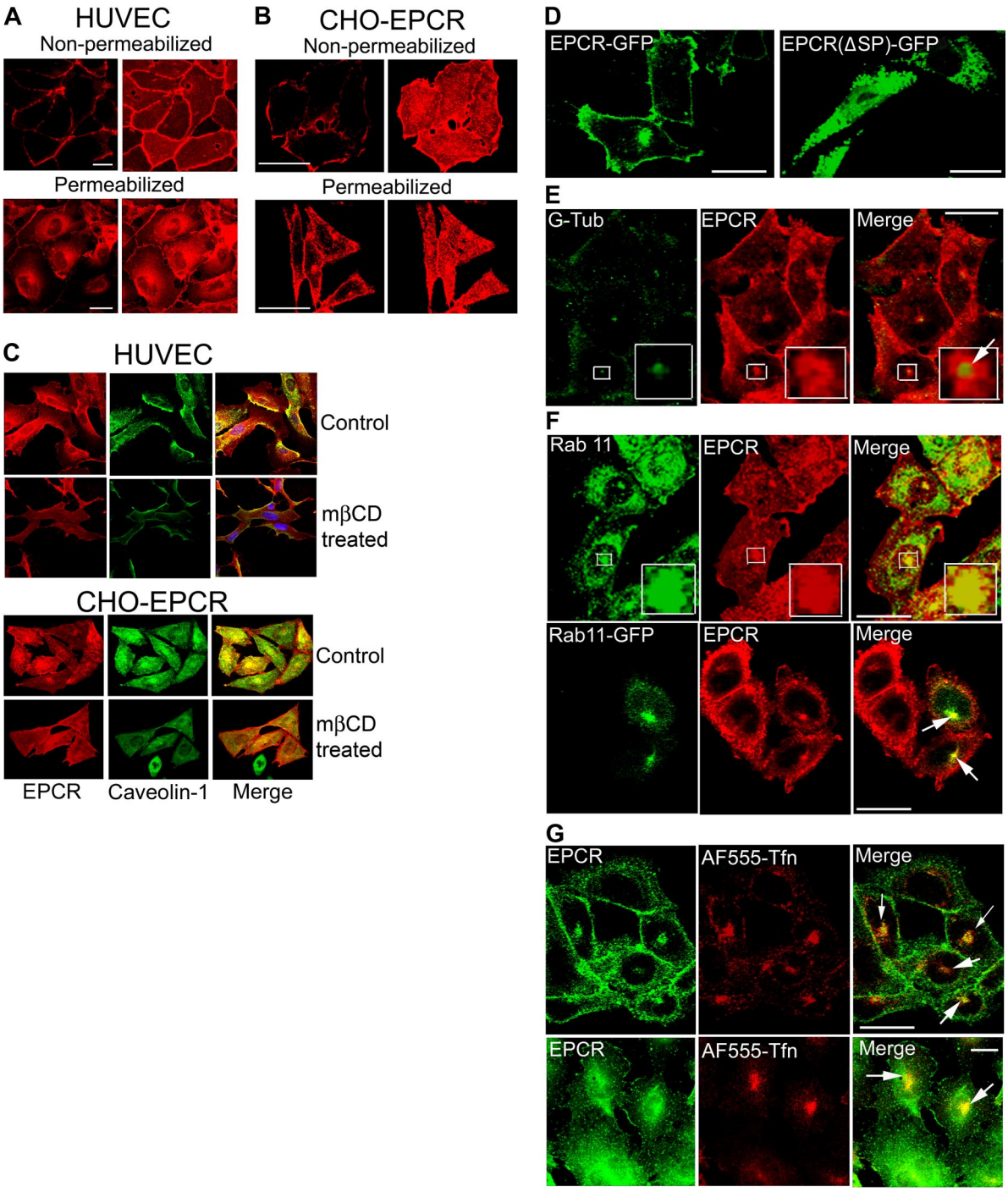

Figure 1. Cellular distribution of EPCR. (A) Confluent monolayers of HUVECs, nonpermeabilized or permeabilized with 0.1% Triton X-100 for 10 minutes, were immunostained with EPCR mAbs (JRK1500, 10 μg/mL), followed by Rhodamine Red-conjugated anti–mouse IgG. Immunofluorescence was analyzed by confocal microscopy. (Left) Images from a single plane of z-stack. (Right) Three-dimensional reconstructed composite images of all z-stacks. (B) CHO-EPCR cells were immunostained with EPCR mAbs as described in panel A. (C) HUVECs (top panel) and CHO-EPCR cells (bottom panel) were first treated with either control vehicle or mβCD (10 mM) for 30 minutes (to deplete the membrane cholesterol) and then permeabilized with 0.1% Triton X-100 for 10 minutes. The permeabilized cells were immunostained with polyclonal anti–human caveolin-1 and EPCR mAbs followed by Oregon Green–labeled anti–rabbit IgG and Rhodamine Red-labeled anti–mouse IgG as secondary reporter antibodies. (Right, merge) Overlay of caveolin-1 and EPCR staining. The images shown were composite images. (D) CHO cells were transfected transiently with full-length EPCR-GFP or EPCR lacking N-terminal signal peptide (EPCR Δsp)–GFP fusion construct, and the expression of green fluorescent fusion product was analyzed by confocal microscopy. (E) CHO-EPCR cells were permeabilized and immunostained with polyclonal anti–γ-tubulin and EPCR mAbs. (Insets) The magnified view of the boxed regions. Arrow represents separation of green and red fluorescence, which indicates that γ-tubulin is not colocalized with EPCR. The presence of EPCR around γ-tubulin indicates that EPCR is localized in the pericentriolar region. (F) CHO-EPCR cells were immunostained either with polyclonal anti-rab11 and EPCR mAb (top panel) or transiently transfected with rab11-GFP and then immunostained with EPCR mAb (bottom). (Insets) Magnified view of the boxed regions. It is known that rab11 also associates with other endosomal compartments and secretory vesicles[19-21]; therefore, rab11 antibodies, in addition to the REC, also stained other intracellular compartments. (G) CHO-EPCR cells (top panel) or HUVECs (bottom panel) were treated with AF555-transferrin (300 nM) for 1 hour and then immunostained with EPCR mAbs. Arrows in the right panel represent the colocalization of EPCR and AF555-trasferrin in the REC. Scale bar represents 15 μm. The REC is not visual in all cells as its position could vary from cell to cell. The REC that is positioned on top of the nucleus may give a false impression that it is localized in the nucleus.

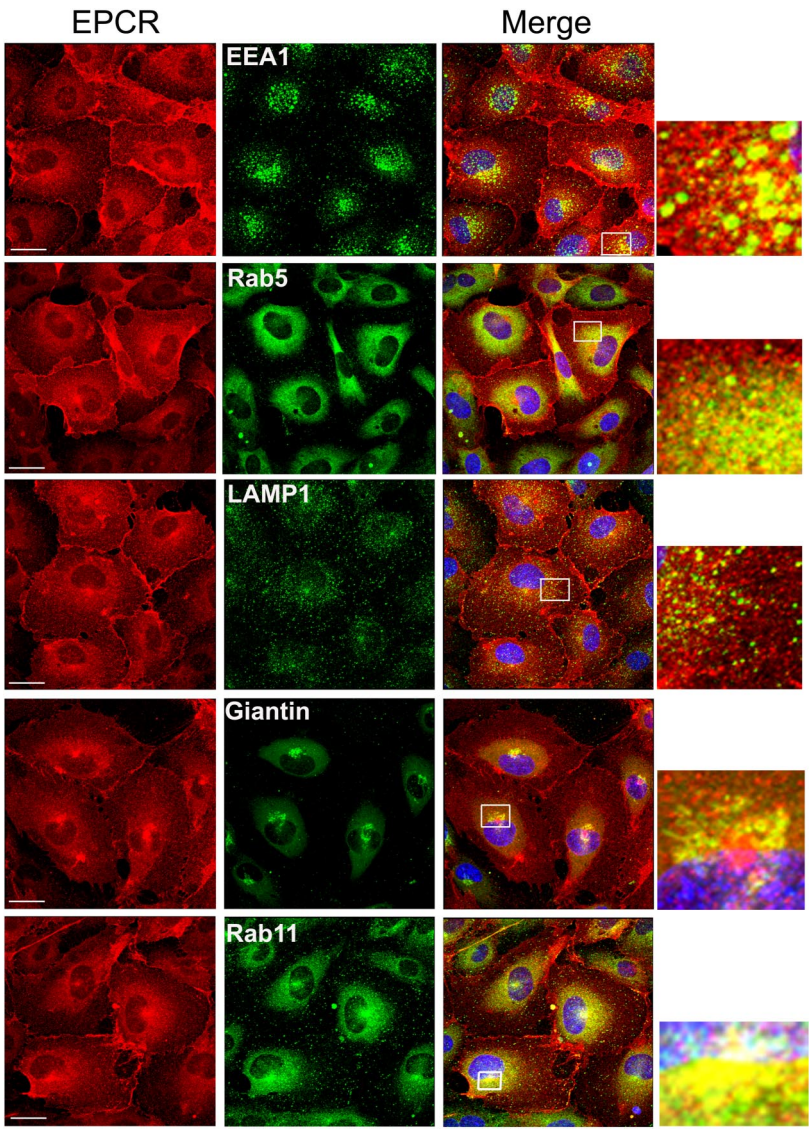

Figure 2. Intracellular distribution of EPCR in endothelial cells. Permeabilized HUVECs were immunostained with EPCR mAbs and an organelle-specific antibody. (Left panel) EPCR-specific staining. (Middle panel) Organelle-specific staining. (Right panel) The overlay image (colocalization) of organelle-specific marker and EPCR. Organelle-specific antibodies used were as follows: anti-EEA1 and anti-rab5 for early endosomes, anti-LAMP1 for lysosomes, Giantin for the Golgi and rab11 for the recycling compartment. A small portion of the merged image, bordered with the white box, was digitally enlarged to illustrate the colocalization.

full-length EPCR (EPCR-GFP) was localized to the cell surface as well as to the juxtanuclear region inside the cell (Figure 1D). In contrast, the signal peptide-deleted EPCR-GFP fusion construct was distributed throughout the cytoplasm but not at the cell surface or at the centrosomal location (Figure 1D). In additional studies, CHO-EPCR cells were immunostained for EPCR as well as γ-tubulin, a centrosomal marker. Although both EPCR and γ-tubulin were localized at the perinuclear vicinity, close examination revealed that EPCR is not colocalized with γ-tubulin (Figure 1E). The pericentriolar localization of EPCR may reflect EPCR localization in a recycling endosomal compartment (REC) as EPCR is colocalized with rab11, a marker for REC (Figure 1F). EPCR localization in the REC was further confirmed by its colocalization with internalized transferrin, which is widely known to enter the recycling compartment after its internalization (Figure 1G).

We next characterized the subcellular distribution of EPCR in endothelial cells by dual immunofluorescence confocal microscopy. HUVECs were immunostained with EPCR mAb and an antibody to an organelle-specific marker protein. A small fraction of EPCR is localized with EEA1 and rab5 in punctuate intracellular structures in the cytoplasm (Figure 2), indicating that a fraction of intracellular EPCR is localized in endosomes. Only a minimal colocalization of EPCR with the lysosomal protein marker, LAMP1, was detected. A partial colocalization of EPCR with Giantin was seen in some but not in all the cells, suggesting a potential localization of EPCR in the Golgi. However, the partial colocalization of EPCR seen with Giantin may reflect an overlap of EPCR in the REC and Giantin in the Golgi, which were localized in spatially distinct compartments. Consistent with this notion, brefeldin treatment, which disrupts the Golgi, did not alter perinuclear localization EPCR (data not shown). Extensive colocalization of EPCR and rab11 in endothelial cells confirms the observation that intracellular EPCR is localized primarily in REC. A similar pattern of subcellular distribution of EPCR was noted in CHO-EPCR cells (supplemental Figure 2).

EPCR mediates FVIIa and APC internalization and undergoes ligand-induced endocytosis

To evaluate EPCR-mediated FVIIa and APC internalization in endothelial cells using immunofluorescence confocal microscopy, HUVECs were exposed to FVIIa or APC (50 nM) conjugated with fluorescent dye AF488 for various time periods at 37°C. At 15 minutes, most of the AF488-FVIIa associated with endothelial cells was at the cell surface. By 30 and 60 minutes, AF488-FVIIa added to HUVECs were internalized and accumulated near a perinuclear location with EPCR (Figure 3A). A similar internalization pattern was also observed with AF488-APC (supplemental Figure 3A). In additional studies, we also analyzed the internalization of FVII and protein C in endothelial cells. The data

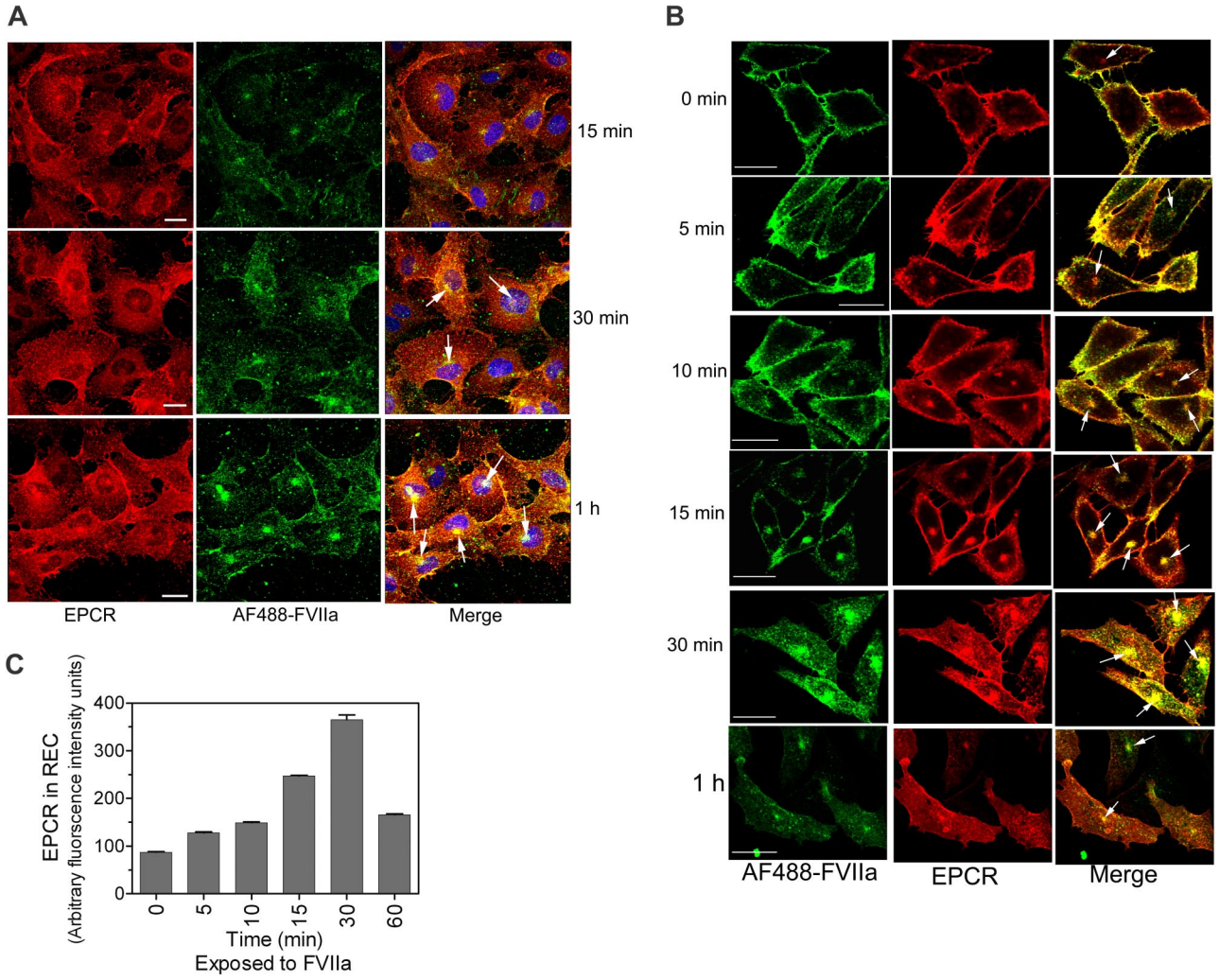

Figure 3. Internalization of FVIIa bound to EPCR. (A) HUVECs were exposed to AF488-FVIIa (50 nM) for 15 minutes, 30 minutes, or 1 hour at 37°C, and then fixed and processed for EPCR immunostaining. (Left) EPCR staining. (Middle) AF488-FVIIa fluorescence. (Right) The overlay image of left and middle panels. Arrows represent the accumulation of AF488-FVIIa with EPCR in the REC. (B) CHO-EPCR cells were exposed to AF488-FVIIa (50 nM) for 1 hour at 4°C. At the end of 1 hour, the supernatant was removed, and the cells were washed quickly with calcium-containing buffer to remove the unbound ligands and then transferred to 37°C to allow internalization of the surface-bound ligands. Various times at 37°C, the cells were fixed, permeabilized, and immunostained with nonblocking EPCR mAb. (Left) AF488-FVIIa. (Middle) EPCR staining. (Right) The merged image of AF488-FVIIa and EPCR. Because the REC could locate at apical, basal, or lateral position to the nucleus, it may not be visible in all sections of the cell. (C) Ligand-induced EPCR accumulation in the REC. CHO-EPCR cells were first incubated with FVIIa (50 nM) at 4°C for 1 hour and then transferred to 37°C. At various times, the cells were fixed, permeabilized, and stained with EPCR mAbs. The pixel density of the fluorescence of EPCR staining in the REC at different time periods was measured using Image suite software (PerkinElmer Life and Analytical Sciences; n = 15 cells or more).

showed that FVII and protein C were internalized in a similar fashion as that of FVIIa and APC (supplemental Figure 3B-C), suggesting that EPCR-mediated endocytosis of its ligands was independent of the protease activity of the ligands.

Endothelial cells that were subjected to temperature fluctuations and repeated washings were prone to loose cell morphology and dissociate readily from the culture dish. Because of this and the limited expression of EPCR on endothelial cells, further experiments to investigate the kinetics of EPCR-mediated FVIIa and APC endocytosis and their recycling were carried out in CHO-EPCR cells. CHO-EPCR cells were first exposed to AF488-FVIIa or AF488-APC for 1 hour at 4°C to allow FVIIa or APC binding to EPCR. Thereafter, the unbound ligands were removed by removing the supernatant and washing the cells in calcium-containing buffer, and then transferred to 37°C to initiate the internalization process. Both AF488-FVIIa and AF488-APC bound to CHO-EPCR cell surface at 4°C and the bound ligand was extensively colocalized with the EPCR at the cell surface (Figure 3B, supplemental Figure 4; correlation coefficient of colocalization for FVIIa and EPCR, 0.939 ± 0.008, $n = 10$). After 5 minutes at 37°C, most of the ligand was still found at the cell surface; the traces of ligands that were internalized at this time were localized primarily beneath the plasma membrane. However by 10 to 15 minutes at 37°C, a clear detectable accumulation of AF488-FVIIa and AF488-APC in the REC was noted. The maximum amount of AF488-FVIIa and AF488-APC accumulated in the REC by 30 minutes (Figure 3B, supplemental Figure 4). Along with the ligands, the amount of EPCR in the REC was also increased significantly during this time period (Figure 3C). EPCR and the internalized ligands were colocalized extensively in the REC at 30 minutes. Thereafter, the amount of both the ligand and the receptor accumulated in the REC was decreased, suggesting sorting of the ligand and the receptor from the REC to the cell surface or lysosomal degradation pathway. FVIIa and APC internalization was very specific to the EPCR-mediated process as we found no detectable internalization/accumulation of AF488-FVIIa or AF488-APC if the cell surface EPCR was blocked with EPCR blocking mAb (JRK1494) before adding AF488-FVIIa or AF488-APC (data not shown). We also

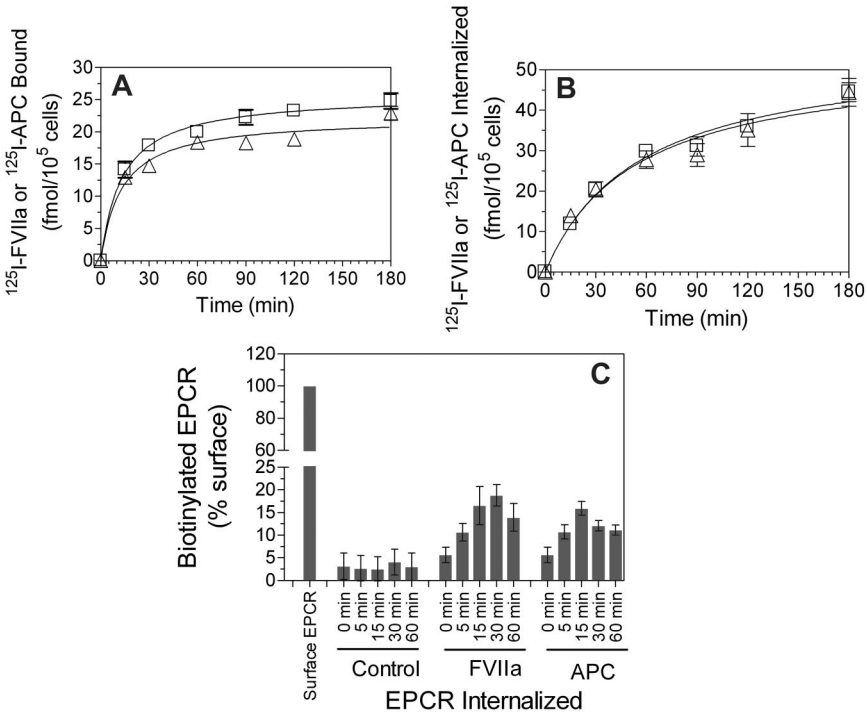

Figure 4. FVIIa or APC binding to EPCR leads to internalization of both the ligand and the receptor. CHO-EPCR cells were incubated with ^{125}I-labeled FVIIa (□) or APC (Δ; 10 nM) for various time intervals at 37°C, and the amount of ^{125}I-labeled proteins associated with the cell surface (A) and internalized (B) was measured. Data are mean ± SEM (n = 4-5). (C) CHO-EPCR cells were surface-labeled with sulfo-NHS-SS-biotin at 4°C and then incubated at 37°C for various time periods with a control buffer or the buffer containing FVIIa or APC (10 nM). The cells were then treated with the reducing agent to remove biotin label from the cell surface, lysed, and immunoprecipitated with anti-EPCR antibody. The immunoprecipitated samples were subjected to SDS-PAGE followed by immunoblot analysis with antibiotin antibodies to detect the internalized EPCR. Biotinylated EPCR signal was quantified by densitometry. Biotinylated EPCR signal detected in the cells immediately after the biotinylation was taken as 100%. The values shown in the figure represent mean ± SEM (n = 3).

analyzed the internalization of active site-inhibited FVIIa and active site-inhibited APC. Consistent with the notion that EPCR-mediated endocytosis and recycling of FVIIa or APC are independent of its protease activity, we found no differences between the proteolytically active ligands and the inactive ligands in their binding to EPCR or their subsequent internalization and accumulation in the REC (supplemental Figures 5A-B).

The EPCR-mediated internalization of FVIIa and APC were also noted using radiolabeled ligands. ^{125}I-FVIIa or ^{125}I-APC (10 nM) added to CHO-EPCR cells was internalized in a time-dependent manner (Figure 4B). There were no significant differences in the rate of FVIIa and APC internalization. Evidence for the ligand-induced internalization of EPCR was also obtained in experiments where cell surface proteins were biotinylated by cell-impermeable NHS-SS-biotin and then exposed to FVIIa or APC. Analysis of EPCR immunoprecipitates from cells treated with a control vehicle showed a minimal increase of biotinylated EPCR in the intracellular pool of proteins over the time. However, there was a substantial increase in biotinylated EPCR in the intracellular compartment if the cells were exposed to FVIIa or APC (Figure 4C), indicating that EPCR undergoes endocytosis on binding to its ligands.

Monitoring the internalization of transferrin along with the internalization of the receptor and ligands under the investigation was widely used to characterize the endocytic pathway. Therefore, we investigated steady-state internalization of both AF488-FVIIa and AF555-transferrin simultaneously in CHO-EPCR cells. Five minutes after the addition of AF488-FVIIa and AF555-transferrin, both of them were found in distinctive globular-like structures, early endosomes, in the cytoplasm just beneath the plasma membrane (supplemental Figure 6). At 15 minutes, AF488-FVIIa and AF555-transferrin were localized in distinctive structures near the perinuclear region. This may reflect FVIIa in sorting endosomes and evolving REC. At 30 minutes, AF488-FVIIa and AF555-transferrin were localized in a dense patch at the pericentriolar area, which is the REC. AF488-APC followed a similar endocytic pathway as of AF488-FVIIa.

FVIIa and APC internalize via the dynamin- and caveolae-dependent pathway

To determine the mechanism by which FVIIa and APC internalize, we tested different inhibitors for their ability to block the internalization. First, we determined whether FVIIa and APC internalize via a dynamin-dependent process by inhibiting dynamin-specific GTPase activity with the specific inhibitor, Dynasore. Dynasore treatment markedly attenuated the internalization of FVIIa and APC in CHO-EPCR cells (Figure 5A,D). As expected, inhibition of the dynamin-dependent pathway of internalization completely abolished the internalization of AF555-transferrin.

Next, we analyzed whether FVIIa and APC internalize via a clathrin- or caveolin-1-dependent pathway. Potassium depletion is known to inhibit the formation of clathrin-coated pits[22] and thus widely used to inhibit clathrin-dependent endocytosis. Potassium depletion completely blocked the internalization of transferrin. In contrast, potassium depletion failed to block the internalization of FVIIa or APC (Figure 5B,D). Indeed, we observed an increase in FVIIa and APC internalization in potassium-depleted cells. This could be the result of the presence of Mg^{2+} in the potassium-depletion buffer used in the assay as Mg^{2+} was found to increase the association of FVIIa and APC to EPCR[23] (R.C.N., P.S., L.V.M.R., unpublished data, 2008). To inhibit the caveolar-dependent pathway of internalization, CHO-EPCR cells were first treated with mβCD (10 mM) for 30 minutes to deplete membrane cholesterol, which disrupts caveolae, before adding the ligands. As shown in Figure 4C, cholesterol depletion had no effect on the internalization of transferrin, which was known to be internalized via clathrin-coated pit pathway. In contrast to the lack of effect on transferrin internalization, mβCD treatment markedly inhibited the internalization of FVIIa and APC (Figure 5C-D). Overall, our data suggest that FVIIa and APC internalize via the dynamin- and caveolar-dependent pathway.

Endocytosed FVIIa and APC recycle back to the cell surface

To determine the fate of internalized FVIIa or APC, first AF488-FVIIa or AF488-APC (50 nM) was allowed to internalize in CHO-EPCR cells;

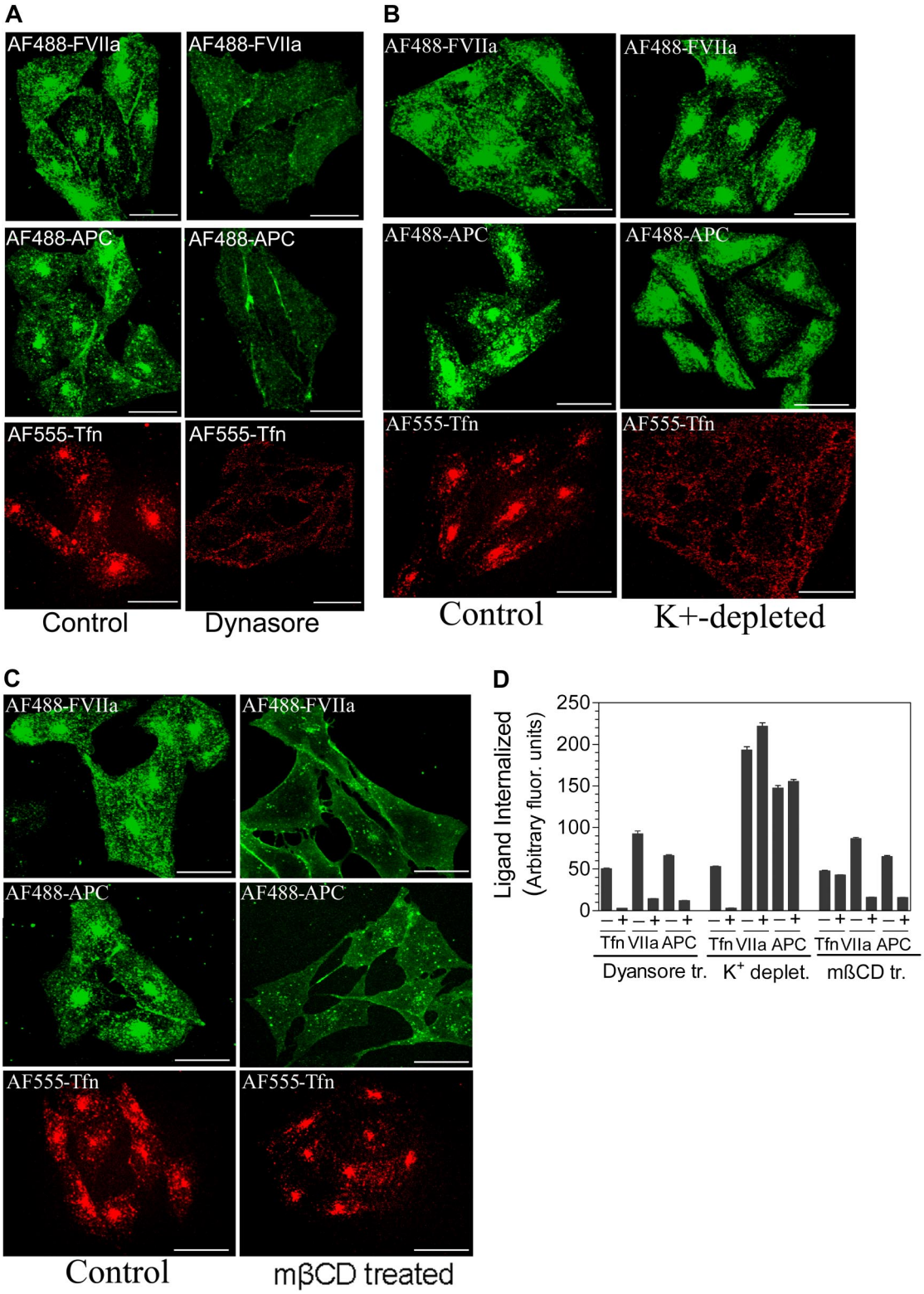

Figure 5. EPCR-mediated internalization of FVIIa and APC is dependent on dynamin and caveolar-mediated endocytosis. (A) CHO-EPCR were treated with a control vehicle (0.25% dimethyl sulfoxide) or Dynasore (80 μM), a specific inhibitor of dynamin GTPase, for 30 minutes. (B) CHO-EPCR cells were treated with control or K^+-depleted buffer to inhibit clathrin-dependent endocytosis. (C) CHO-EPCR cells were treated with a control vehicle or mβCD (10 mM) for 30 minutes to disrupt caveolae. After aforementioned specific treatments, the cells were exposed to AF488-FVIIa (50 nM), AF488-APC (50 nM), or AF555-transferrin (Tfn; 300 nM) for 1 hour at 37°C. The fluorescence of internalized ligands was analyzed by confocal microscopy. The extent of internalization was quantified (D) by measuring the fluorescence intensity in the defined area corresponding to the recycling compartment. To identify the recycling compartment for the quantification, the cells were immunostained with EPCR mAbs (mean ± SEM, n = 15-25 cells).

and then after removing the cell-associated AF488-FVIIa or AF488-APC, the cells were allowed to stand at 37°C for various time periods before they were processed for immunofluorescence microscopy. At 5 minutes, most of the internalized AF488-FVIIa remained concentrated in the REC. Between 15 and 30 minutes, FVIIa in the REC was decreased and appeared throughout the cytoplasm in dot-like structures

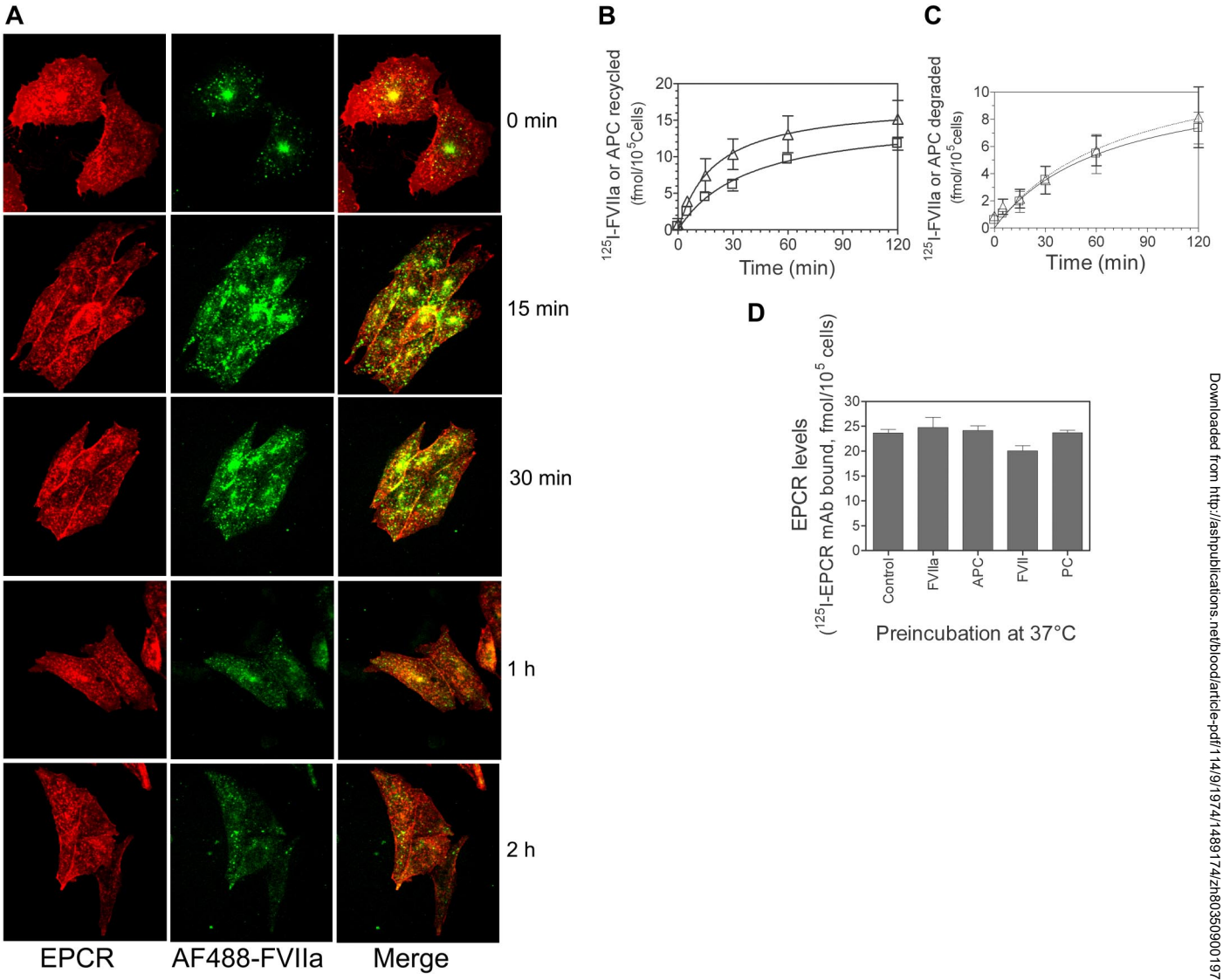

Figure 6. Recycling of internalized FVIIa and EPCR, and the fate of internalized ligands. (A) CHO-EPCR cells were incubated with AF488-FVIIa (50 nM) for 1 hour at 37°C to allow the internalization of FVIIa. Thereafter, the cells were washed with the buffer containing 5 mM ethylenediaminetetraacetic acid to remove the cell surface bound FVIIa, and thereafter the cells were maintained in calcium-containing buffer (buffer B) at 37°C. The fate of internalized FVIIa was monitored by fixing the cells at various times. The fixed cells were permeabilized, stained with EPCR mAbs, and analyzed by confocal microscopy. (B-C) CHO-EPCR cells were exposed to ^{125}I-FVIIa (triangle) or ^{125}I-APC (square), 10 nM, for 2 hours at 37°C, and then the surface associated ^{125}I-labeled ligand was eluted by treating the cells with 0.1 M glycine, pH 2.3, for 3 minutes at the room temperature. The cells were washed with buffer B and allowed to stay at 37°C. At various time intervals, the overlying supernatant medium was removed and precipitated with 10% ice-cold TCA. The radioactivity present in both TCA-precipitable (B) and TCA-soluble fractions (C) was counted. (D) CHO-EPCR cells were incubated with a control buffer or the buffer containing unlabeled FVII, FVIIa, protein C, or APC (100 nM). After 2 hours at 37°C, the unbound ligand was removed, and the monolayers were washed with 0.1 M glycine, pH 2.3, to remove the bound ligand. After washing the monolayers with buffer B, the cells were chilled on ice and incubated with ^{125}I-EPCR mAbs (10 nM) at 4°C for 1 hour. After 1 hour, the unbound radioactivity was removed, the cells were washed, and the total cell lysate was counted for the radioactivity to determine the amount of EPCR mAbs bound to the cells.

(Figure 6A). At these time intervals, we also observed the appearance of AF488-FVIIa at the cell surface. AF488-FVIIa fluorescence in the cytoplasm was decreased markedly between 1 and 2 hours; and at the end of 2 hours, no AF488-FVIIa was detectable in the cytoplasm. However, there was no corresponding increase in AF488-FVIIa fluorescence at the cell surface. It is possible that most of the internalized FVIIa recycled back to the cell surface, but this recycled FVIIa readily dissociates from the cell surface. To test this possibility, we examined the recycling of internalized FVIIa and APC using radiolabeled ligands. ^{125}I-FVIIa or ^{125}I-APC (10 nM) was allowed to internalize for 2 hours at 37°C, and then the surface-associated ^{125}I-labeled protein was removed by low pH buffer wash (0.1 M glycine, pH 2.3). Thereafter, the cells were maintained in Ca^{2+}-containing buffer. At various time intervals, the amount of radioactivity released into overlying medium or associated with the cell surface was evaluated. There was a time-dependent increase in ^{125}I-FVIIa or ^{125}I-APC, both intact (trichloroacetic acid [TCA]–precipitable) and degraded (TCA-soluble) in the overlying media (Figure 6B-C). The majority of the FVIIa or APC released into overlying media was intact (compare Figure 6B-C). SDS-PAGE analysis of the overlying media confirmed this. FVIIa secreted into overlying media is functionally active (data not shown; APC activity was not tested). We found no significant increase in the cell-associated ^{125}I-FVIIa or ^{125}I-APC (varied between 2 and 3 fmol/10^5 cells at different time intervals), indicating that most of the ^{125}I-FVIIa or ^{125}I-APC was released into overlying medium. To determine whether EPCR was depleted from the cell surface in the process of FVIIa or APC internalization or the EPCR endocytosed with the ligands completely recycled back to the cell surface, CHO-EPCR cells were incubated with

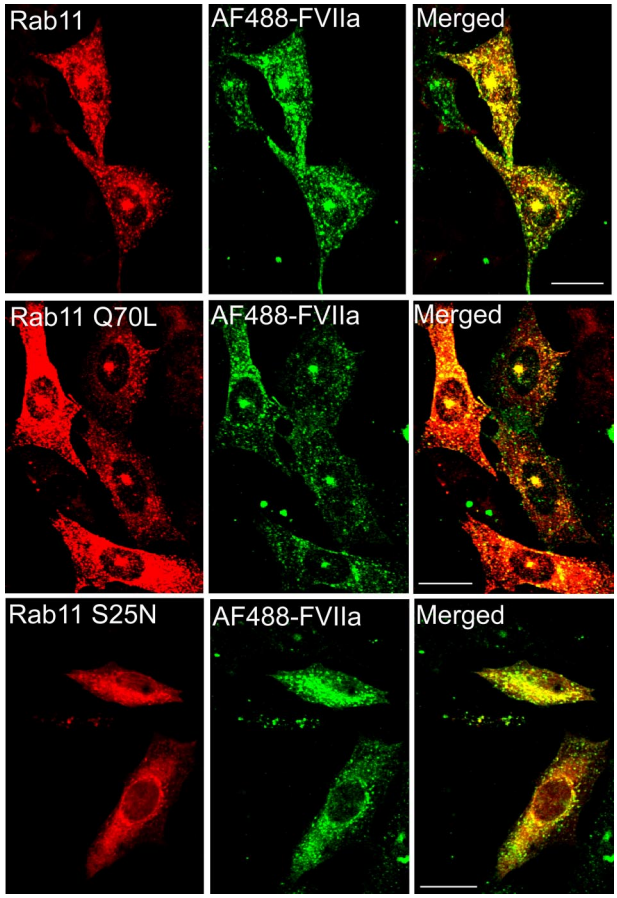

Figure 7. Involvement of rab11 in sorting the internalized FVIIa into the recycling compartment. CHO-EPCR cells were transiently transfected with wild-type rab11, constitutively active rab11 (Q70L), or dominant negative rab11 (S25N), and the transfected cells were exposed to AF488-FVIIa for 1 hour at 37°C. The cells were fixed, permeabilized, and immunostained for rab11. The fluorescence of internalized AF488-FVIIa and immunofluorescence of rab11 were analyzed by confocal microscopy.

a control buffer or the buffer containing unlabeled FVII, FVIIa, protein C, or APC (100 nM) for 2 hours at 37°C. As shown in Figure 6D, exposure of the cells with EPCR ligands failed to reduce EPCR levels at the cell surface, indicating that endocytosed EPCR recycled back fully to the cell surface.

Rab11 regulates FVIIa recycling

Rab11 is localized to REC and plays an important role in the internalization and recycling through the REC.[19,24] To examine the involvement of rab11 in FVIIa and APC internalization and recycling, CHO-EPCR cells were transiently transfected with wild-type, constitutively active (rab11 Q70L) or dominant negative (rab11 S25N) rab11, and the transfected cells were exposed to AF488-FVIIa or AF488-APC (50 nM). In cells expressing the wild-type and constitutively active form of rab11, the internalized AF488-FVIIa accumulated in the REC (Figure 7). In cells transfected with dominant negative rab11S25N, AF488-FVIIa did not accumulate in the REC but distributed throughout the cytoplasm. These data indicate that rab11 regulates processing of the internalized FVIIa into the REC. Similar findings were noted for APC (data not shown).

EPCR-mediated endocytosis/recycling: potential physiologic significance

To investigate the potential physiologic role for EPCR-mediated endocytosis and recycling, we first examined whether EPCR-mediated endocytosis facilitates FVIIa transport across the cell, from the apical to the basal side. As shown in Figure 8A, ^{125}I-FVIIa (10 nM) added to the apical side of confluent monolayers of CHO-EPCR cells grown in a transwell chamber was transported to the basal side in a time-dependent manner. Relative to BSA, which was used as a measure for paracellular transfer (membrane integrity) or fluid-phase transcytosis, 4-fold or more ^{125}I-FVIIa was transported to the basal side. FVIIa transcytosis is EPCR-dependent as EPCR-blocking mAb attenuated the transport of FVIIa. Consistent with this, the transport of FVIIa is significantly lower in wild-type CHO cells compared with CHO-EPCR cells. Trichloroacetic acid precipitation or SDS-PAGE analysis of the basal medium revealed that the majority of FVIIa transported to the basal side is intact (data not shown). Similar results were obtained with HUVECs, although the data were not as robust as observed with CHO-EPCR cells.

To investigate whether the afore-described mechanism operates in vivo, AF488-FVII or AF488-protein C (10 μg/mice) was administered to mice via tail injection, and their distribution in the blood vessel was analyzed using immunohistochemistry. As shown in Figure 8B, both FVIIa and APC administered to mice were localized not only on endothelial cells lining blood vessels but also in the adventitia and extravascular tissue, suggesting that FVIIa and APC bound to endothelium could enter extravascular space.

We also investigated whether blocking of FVIIa binding to EPCR in vivo impairs FVIIa clearance from the circulation. Before administering human FVIIa to mice, first we tested whether human FVIIa binds to mouse EPCR and this binding could be blocked by mEPCR blocking mAb. As shown in supplemental Figure 7, the amount of human FVIIa bound to 293E cells stably transfected with mouse EPCR was 3-fold higher than the amount of FVIIa associated with the wild-type cells. FVIIa binding to mEPCR-expressing cells is completely attenuated by mEPCR-blocking antibody (mAb 1560) but not by nonblocking antibody (mAb 1567). Next, ^{125}I-FVIIa (5 μg/kg body weight) was administered to mice via tail vein, and its clearance was monitored by measuring the recovery of radioactivity in plasma at various times. ^{125}I-FVIIa was cleared from the circulation in a biphasic manner with $t_{1/2}$ of 19.9 plus or minus 0.075 minutes in the first phase (α-phase) and 209 plus or minus 4 minutes in the later phase (β-phase). Administration of EPCR nonblocking antibodies had no significant effect on FVIIa clearance ($t_{1/2}$ of α-phase, 16.5 ± 2.5 minutes; β-phase, 217 ± 16 minutes). In contrast, blocking EPCR with the blocking antibodies significantly reduced FVIIa clearance from the circulation, particularly in the α-phase ($t_{1/2}$ of α-phase, 30.7 ± 2.13 minutes; β-phase 256 ± 52; n = 3).

Discussion

To gain the insights into the mechanism involved in EPCR endocytosis and the intracellular itinerary of the internalized ligands, we first characterized the cellular localization of EPCR. In this study, we used endothelial cells, the cells that express EPCR in vivo, and a heterologous expression system (CHO cells stably transfected with EPCR), which allows us to obtain more robust data and mechanistic information. EPCR in HUVECs and CHO-EPCR cells was predominantly localized on the cell surface with a small pool of EPCR in intracellular compartments. At the cell surface, EPCR appeared to be localized primarily in discrete plasma membrane microdomains. A high degree of EPCR colocalization with caveolin-1 in distinctive membrane microdomains

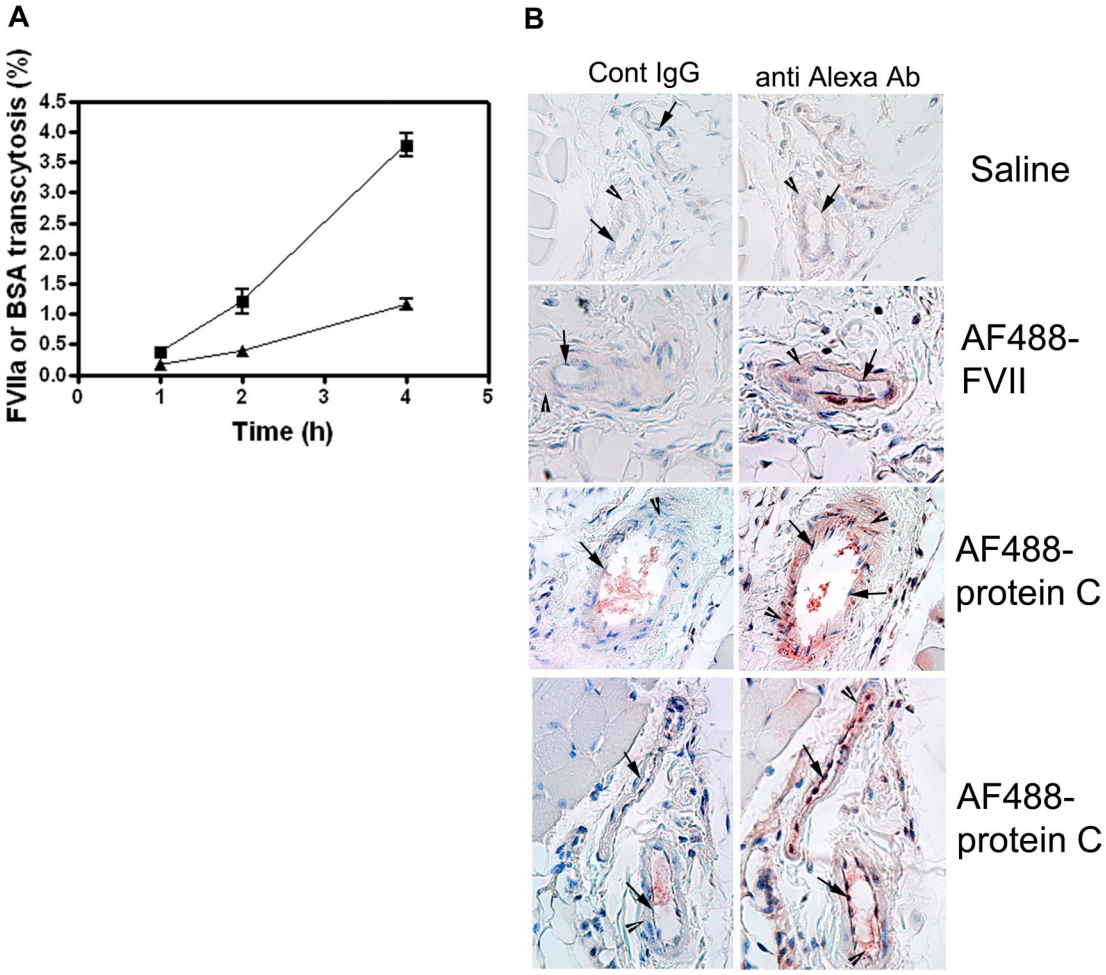

Figure 8. EPCR-mediated FVIIa transcytosis. (A) CHO-EPCR cells cultured in transwells were treated with control vehicle or EPCR blocking mAb (10 μg/mL) for 30 minutes. Thereafter, ^{125}I-FVIIa (10 nM) and BSA coupled to Evans Blue (0.67 mg/mL) were added to the upper chamber, and the cells were allowed to stay in the CO_2 incubator. At various times, a small aliquot was removed from the bottom chamber and counted for the radioactivity and measured absorbance at 650 nm to monitor the transfer of FVIIa and BSA, respectively, to the bottom chamber. The data shown in the figure represent EPCR-specific FVIIa transport (n = 3). BSA transfer in CHO-EPCR cells treated with control vehicle or EPCR blocking mAbs is very similar. (B) C57BL/6 mice were injected with saline control (100 μL), AF488-FVII, or AF488-protein C (10 μg/mice in 100 μL saline) via tail vein. One hour after the injection, the mice were exsanguinated, and various tissues were collected into Excel fixative. Bone-joint tissue was sectioned (5-μm thickness) and immunostained with anti-AF488 antibodies to localize the administered FVII and protein C. [↓] represents endothelial lining; [➤], adventitia and extravascular tissue.

suggests that EPCR is localized in caveolae. The present data are consistent with earlier observations showing that EPCR was fractionated into the low buoyant density membrane fractions where caveolin-1 and other proteins associated with lipid rafts and caveolae were found.[25,26] EPCR localization in caveolae along PAR1 is thought to play an important role in APC-mediated cell signaling.[27] The caveolar localization of EPCR may also facilitate regulated release of EPCR from cells.[28]

Most of the intracellular EPCR in both HUVECs and CHO-EPCR cells was concentrated juxtanuclearly at a dense cytoplasmic spot, an expected site of the centrosome or recycling compartment. Interestingly, earlier studies showed that cDNA-encoding murine centrosomal protein CCD41 was identical with the cDNA for murine EPCR.[11] Further, using GFP technology, it was shown that the transfection of Ehrlich ascites tumor cells with GFP fusion construct containing full-length CCD41 cDNA resulted in expression of the fusion protein at the cell surface, whereas the GFP-fusion product lacking the signal peptide sequence was exclusively incorporated into a small perinuclear structure, which is the site of the centrosome.[11] Based on these data, it was hypothesized that one single mRNA encodes the centrosomal protein CCD41 and the EPCR, and the posttranslational modification, namely, the deletion of signal peptide, is decisive for the centrosomal location of the protein while the unprocessed protein is incorporated into the cell membrane.[11] Our present data fail to support the aforementioned hypothesis, at least in the cell model systems we used. Transfection of CHO cells with full-length human EPCR fused with EGFP resulted in expression of the fusion protein at the plasma membrane as well as in the perinuclear compartment. Further, transfection of CHO cells with the signal sequence-deleted EPCR mutant resulted in diffused expression of the fusion product throughout the cytoplasm and not targeted to the centrosomal location. In CHO cells and in many other cell types, the recycling compartment resides around the centrosome, so-called pericentriolar recycling compartment[19] thus; it is probable that the EPCR staining we observed in the perinuclear compartment represented EPCR in the recycling compartment. Consistent with this notion, we observed a high degree of EPCR colocalization with rab11 and internalized transferrin, markers for the recycling endosomes, in the perinuclear compartment. At present, it is unclear whether the observed difference between the present study and the earlier study on the localization of intracellular EPCR reflects a real difference between human and murine EPCR gene products.

The presence of EPCR in the early endosomes and the recycling compartment in untreated cells suggests that EPCR may be constitutively recycling. Although we were unable to obtain convincing evidence for the constitutive recycling of EPCR, one cannot exclude the possibility of very fast internalization of EPCR constitutively coupled with rapid recycling back to the cell surface, which cannot be captured by the present methodology. An earlier preliminary report suggested that EPCR was constitutively translocated into the nucleus.[29] In the present study, we failed to detect any translocation of EPCR into the nucleus, either constitutively or on its occupancy by APC or FVIIa. The reason for the discrepancy between our present data and the earlier finding was unclear. Differences in cell model systems and/or experimental methodologies could have contributed to the difference. It is also conceivable that EPCR localized in the juxtanuclear position at the top or bottom of the nucleus might have given an appearance that EPCR was in the nucleus.

It had been speculated that EPCR may internalize APC and translocate it into the nucleus, which in turn could directly modulate the gene expression.[29,30] It had been reported in preliminary studies that APC and not protein C was translocated into the nucleus.[29] The data presented herein clearly show that both APC and FVIIa bound to EPCR were internalized rapidly and in a time-dependent fashion. However, we found no evidence that the internalized ligands were transported into the nucleus. The internalized FVIIa and APC, along the endocytosed EPCR, were sorted into the recycling compartment. This was evident as the internalized FVIIa and APC followed the same route as the internalized transferrin, which was known to enter the sorting endosomes after the internalization and then to the recycling endosomes.[19,31] A high degree of colocalization of the internalized FVIIa or APC with transferrin, a reliable marker for the recycling endosome, further supports this conclusion. We observed no detectable differences in the internalization and trafficking of FVIIa and APC or the zymogen forms of these enzymes, that is, FVII and protein C. Consistent with this finding, inactivation of the protease activity of FVIIa and APC had no effect on their internalization and trafficking. It is unknown at present whether an injury to the endothelium could alter or influence the EPCR-mediated internalization and trafficking of its ligands. It is interesting to note that preliminary studies from Thiyagarajan et al[30] showed that APC added to brain endothelial cells appeared to be transported intracellularly and into the nucleus under hypoxic conditions, whereas it stayed on the cell surface in normoxic condition. These data need to be confirmed.

Endocytosis of EPCR was found to be mediated predominantly via the dynamin- and caveolin-1-dependent mechanism. Once internalized, most of the EPCR and its ligands were targeted from the sorting endosomes to the recycling compartment as we could see a clear, time-dependent accumulation of EPCR and its ligands in the morphologically distinct pericentriolar compartment. From this compartment, both EPCR and the ligands were rapidly transported back to the cell surface. This was evident from the marked decrease in FVIIa and EPCR levels in the recycling compartment between 30 and 60 minutes after the initiation of the endocytic process. This could explain why there was no decrease in EPCR levels at the cell surface even after prolonged incubation with FVIIa or APC. FVIIa or APC that was recycled back to the cell surface was intact, and most of it was secreted into overlying medium rather than associating with the EPCR on the cell surface. This is expected because the affinity of FVIIa or APC to EPCR was in the nanomolar range (40-100 nM). Although we were unable to detect any internalized FVIIa or APC in lysosomes, it seemed that some of the internalized FVIIa or APC was released from the EPCR, probably in the sorting endosomes, and targeted to degradation, as we could see a time-dependent increase in degraded (TCA-soluble) FVIIa or APC in the overlying medium after their internalization.

Small GTPases of the rab family play a critical role in the regulation of intracellular trafficking of receptor and ligand complexes.[32] Rab11 GTPase appears to regulate traffic coming from the sorting endosomes to the recycling endosome.[19] Transfection of CHO-EPCR cells with a rab11 GTPase-deficient mutant, rab11S25N, inhibited the accumulation of the internalized FVIIa (or APC) and EPCR in the recycling compartment and dispersed the internalized ligand throughout the cytoplasm. The blockade of the transport of the internalized ligands to the recycling compartment appeared to impair their transport back to the cell surface as the increased levels of internalized FVIIa and APC were accumulated throughout the cytoplasm.

Although the physiologic importance of FVIIa binding to EPCR is yet to be established, the preliminary unpublished studies of the authors' laboratory (S.G., L.V.M.R., March 2008) show that FVII levels in plasma are significantly lower in EPCR overexpressing mice, whereas the levels are slightly elevated in EPCR-deficient mice, indicating that FVII/FVIIa does interact with EPCR in vivo. A large body of evidence exists showing that endothelial transcytosis plays an important role in the regulation of molecular exchanges between blood and peripheral tissues and participates in a variety of vascular diseases.[33,34] Based on our present data, it is possible that EPCR-mediated endocytosis/recycling may facilitate transcytosis of protein C and FVII in vivo, thus transporting protein C/APC and FVII/FVIIa from the lumen of blood vessels to the subendothelial space. This could facilitate FVII/FVIIa coming into contact with tissue factor (TF) in the absence of vascular injury. Formation of traces of TF-FVIIa complexes in subendothelial space may prime TF-dependent blood coagulation or propagate basal TF-FVIIa signaling. Several nonendothelial cells, such as smooth muscle cells[35] and keratinocytes,[36] express thrombomodulin and generation of thrombin in extravascular tissue can have devastating consequences. EPCR-mediated transport of protein C/APC to the basolateral side could regulate thrombin generation in extravascular space. In addition to facilitating the receptor-mediated transcytosis, EPCR-mediated FVIIa endocytosis may also play a role in FVIIa clearance in vivo. However, because a majority of the internalized FVIIa appears to recycle back to the cell surface, it is doubtful that EPCR-mediated FVIIa internalization could account fully for FVIIa clearance. Consistent with this hypothesis, blocking the EPCR with specific antibodies significantly delayed the clearance of FVIIa, particularly in the early phase, but did not completely attenuate FVIIa clearance in mice. Because FVII circulates in plasma at a 7-fold lower concentration than protein C (10 vs 70 nM) and exhibits a similar affinity to EPCR,[9] it is doubtful that EPCR-mediated FVIIa endocytosis plays the predominant role in FVIIa clearance in normal physiologic conditions. However, in hemophilia therapy where large doses of FVIIa are administered, FVIIa levels may be elevated close to protein C levels in blood.[37] Under these conditions, EPCR-mediated FVIIa endocytosis may play a major role in removing FVIIa from the circulation.

In conclusion, the present data provide a detailed characterization of EPCR distribution in endothelial cells and a heterologous expression system, and demonstrate that EPCR occupancy by it ligands, FVIIa or APC, results in the internalization of the receptor-ligand complex. Although it is conceivable that the cell model systems may not truly mimic intact endothelial cells on the vessel wall, overall the data presented herein provide a strong indication that EPCR-mediated

endocytosis/recycling may play a role in the transport of its ligands across the endothelial cell barrier and/or their catabolism.

Acknowledgments

The authors thank Gary Ferrel from the laboratory of C.T.E. for many shipments of the reagents and Joshua Atkinson, a summer student intern, who provided technical assistance in constructing EPCR-GFP fusion constructs.

This work was supported by the National Institutes of Health (grant HL 58869, L.V.M.R.; grant HL 65500, U.R.P.). C.T.E. is an investigator of the Howard Hughes Medical Institute.

Authorship

Contribution: R.C.N. performed all experiments involving immunofluorescence confocal microscopy, analyzed the data, compiled the figures, and wrote the first draft of the manuscript; P.S. performed radiolabeling and cell surface biotinylation experiments and contributed to the preparation of the manuscript; S.G. performed FVIIa clearance studies in mice; R.G. performed immunohistochemistry studies in mice; C.T.E. provided the critical reagents, advised on the research design, and contributed to manuscript preparation; U.R.P. participated in the research design, generated EPCR-GFP fusion constructs, and contributed to manuscript preparation; and L.V.M.R. designed the research, supervised all the experiments, analyzed the data, and prepared the manuscript.

Conflict-of-interest disclosure: The authors declare no competing financial interests.

Correspondence: L. Vijaya Mohan Rao, Center for Biomedical Research, University of Texas Health Science Center at Tyler, 11937 US Hwy 271, Tyler, TX 75708; e-mail: Vijay.Rao@uthct.edu.

References

1. Regan LM, Stearns-Kurosawa DJ, Kurosawa S, et al. The endothelial cell protein C receptor: inhibition of activated protein C anticoagulant function without modulation of reaction with proteinase inhibitors. *J Biol Chem.* 1996;271(29):17499-17503.
2. Laszik Z, Mitro A, Taylor FB Jr, Ferrell G, Esmon CT. Human protein C receptor is present primarily on endothelium of large blood vessels: implications for the control of the protein C pathway. *Circulation.* 1997;96(10):3633-3640.
3. Stearns-Kurosawa DJ, Kurosawa S, Mollica JS, Ferrell GL, Esmon CT. The endothelial cell protein C receptor augments protein C activation by the thrombin-thrombomodulin complex. *Proc Natl Acad Sci U S A.* 1996;93(19):10212-10216.
4. Esmon CT. The endothelial protein C receptor. *Curr Opin Hematol.* 2006;13(5):382-385.
5. Riewald M, Petrovan RJ, Donner A, Mueller BM, Ruf W. Activation of endothelial cell protease activated receptor 1 by protein C pathway. *Science.* 2002;296(5574):1880-1882.
6. Cheng T, Liu D, Griffin JH, et al. Activated protein C blocks p53-mediated apoptosis in ischemic human brain endothelium and is neuroprotective. *Nat Med.* 2003;9(3):338-342.
7. Feistritzer C, Riewald M. Endothelial barrier protection by activated protein C through PAR1-dependent sphingosine 1-phosphate receptor-1 crossactivation. *Blood.* 2005;105(8):3178-3184.
8. Ludeman MJ, Kataoka H, Srinivasan Y, et al. PAR1 cleavage and signaling in response to activated protein C and thrombin. *J Biol Chem.* 2005;280(13):13122-13128.
9. Ghosh S, Pendurthi UR, Steinoe A, Esmon CT, Rao LV. Endothelial cell protein C receptor acts as a cellular receptor for factor VIIa on endothelium. *J Biol Chem.* 2007;282(16):11849-11857.
10. Preston RJ, Ajzner E, Razzari C, et al. Multifunctional specificity of the protein C/activated protein C GLA domain. *J Biol Chem.* 2006;281(39):28850-28857.
11. Rothbarth K, Dabaghian AR, Stammer H, Werner D. One single mRNA encodes the centrosomal protein CCD41 and the endothelial cell protein C receptor (EPCR). *FEBS Lett.* 1999;458(1):77-80.
12. Li W, Zheng X, Gu J, et al. Overexpressing endothelial cell protein C receptor alters the hemostatic balance and protects mice from endotoxin. *J Thromb Haemost.* 2005;3(7):1351-1359.
13. Rao LVM, Bajaj SP. Purification of human factor VII utilizing O-(diethylaminoethyl)-Sephadex and Sulfopropyl-Sephadex chromatography. *Anal Biochem.* 1984;136(2):357-361.
14. Qu D, Wang Y, Song Y, Esmon NL, Esmon CT. The Ser219→Gly dimorphism of the endothelial protein C receptor contributes to the higher soluble protein levels observed in individuals with the A3 haplotype. *J Thromb Haemost.* 2006;4(1):229-235.
15. Iakhiaev A, Pendurthi UR, Rao LVM. Active site blockade of factor VIIa alters its intracellular distribution. *J Biol Chem.* 2001;276(49):45895-45901.
16. Le DT, Rapaport SI, Rao LVM. Relations between factor VIIa binding and expression of factor VIIa/tissue factor catalytic activity on cell surfaces. *J Biol Chem.* 1992;267(22):15447-15454.
17. Mandal SK, Pendurthi UR, Rao LV. Cellular localization and trafficking of tissue factor. *Blood.* 2006;107(12):4746-4753.
18. Mandal SK, Pendurthi UR, Rao LV. Tissue factor trafficking in fibroblasts: involvement of protease-activated receptor-mediated cell signaling. *Blood.* 2007;110(1):161-170.
19. Ullrich O, Reinsch S, Urbe S, Zerial M, Parton RG. Rab11 regulates recycling through the pericentriolar recycling endosome. *J Cell Biol.* 1996;135(4):913-924.
20. Urbé S, Huber LA, Zerial M, Tooze SA, Parton RG. Rab11, a small GTPase associated with both constitutive and regulated secretory pathways in PC12 cells. *FEBS Lett.* 1993;334(2):175-182.
21. Goldenring JR, Soroka CJ, Shen KR, et al. Enrichment of rab11, a small GTP-binding protein, in gastric parietal cells. *Am J Physiol.* 1994;267(2 pt 1):G187-G194.
22. Larkin JM, Brown MS, Goldstein JL, Anderson R. Depletion of intracellular potassium arrests coated pit formation and receptor-mediated endocytosis in fibroblast. *Cell.* 1983;33(1):273-285.
23. Fukudome K, Kurosawa S, Stearns-Kurosawa DJ, et al. The endothelial cell protein C receptor cell surface expression and direct ligand binding by the soluble receptor. *J Biol Chem.* 1996;271(29):17491-17498.
24. Ren M, Xu G, Zeng J, et al. Hydrolysis of GTP on rab11 is required for the direct delivery of transferrin from the pericentriolar recycling compartment to the cell surface but not from sorting endosomes. *Proc Natl Acad Sci U S A.* 1998;95(11):6187-6192.
25. Bae JS, Yang L, Rezaie AR. Receptors of the protein C activation and activated protein C signaling pathways are colocalized in lipid rafts of endothelial cells. *Proc Natl Acad Sci U S A.* 2007;104(8):2867-2872.
26. Xu J, Liaw PCY, Esmon CT. A novel transmembrane domain of the EPCR dictates receptor localization of sphingolipid-cholesterol high regions on plasma membrane which EPCR palmitoylation modulates intracellular trafficking patterns. *Thromb Haemost.* 1999;(suppl):2195a.
27. Bae JS, Yang L, Rezaie AR. Lipid raft localization regulates the cleavage specificity of protease activated receptor 1 in endothelial cells. *J Thromb Haemost.* 2008;6(6):954-961.
28. Xu J, Qu D, Esmon NL, Esmon CT. Metalloproteolytic release of endothelial cell protein C receptor. *J Biol Chem.* 1999;275(8):6038-6044.
29. Xu J, Esmon CT. Endothelial cell protein C receptor (EPCR) is constitutively translocated into the nucleus and also mediates activated protein C, but not protein C, nuclear translocation. *Thromb Haemost.* 1999;(suppl):652a.
30. Thiyagarajan M, Cheng T, Zlokovic BV. Endothelial cell protein C receptor: role beyond endothelium? *Circ Res.* 2007;100(2):155-157.
31. Maxfield FR, McGraw TE. Endocytic recycling. *Nat Rev Mol Cell Biol.* 2004;5(2):121-132.
32. Zerial M, McBride H. Rab proteins as membrane organizers. *Nat Rev Mol Cell Biol.* 2001;2(2):107-117.
33. Frank PG, Pavlides S, Lisanti MP. Caveolae and transcytosis in endothelial cells: role in atherosclerosis. *Cell Tissue Res.* 2009;335(1):41-47.
34. Predescu SA, Predescu DN, Malik AB. Molecular determinants of endothelial transcytosis and their role in endothelial permeability. *Am J Physiol Lung Cell Mol Physiol.* 2007;293(4):L823-L842.
35. Yoshii Y, Okada Y, Sasaki S, et al. Expression of thrombomodulin in human aortic smooth muscle cells with special reference to atherosclerotic lesion types and age differences. *Med Electron Microsc.* 2003;36(3):165-172.
36. Mizutani H, Hayashi T, Nouchi N, et al. Functional and immunoreactive thrombomodulin expressed by keratinocytes. *J Invest Dermatol.* 1994;103(6):825-828.
37. Hedner U. Dosing with recombinant factor VIIa based on current evidence. *Semin Hematol.* 2004;41(1 suppl 1):35-39.